SUPPLEMENTARY INFORMATION FOR NMRlipids III: Lipid–Cholesterol Interactions in Atomistic Resolution Molecular Dynamics Simulations

Fernando Favela-Rosales,[†] Peter Heftberger,[‡] Matti Javanainen,[*,¶,§] Jesper J. Madsen,[‖,⊥] Josef Melcr,[¶] Markus Miettinen,[#] O. H. Samuli Ollila,[*,¶,§] Georg Pabst,[‡,@] and Thomas Piggot[△,▽]

†*Departamento de Física, Centro de Investigación y de Estudios Avanzados del IPN, Apartado Postal 14-740, 07000 México D.F., México*

‡*Institute of Molecular Biosciences, Biophysics Division, NAWI Graz, University of Graz, Graz 8010, Austria*

¶*Institute of Organic Chemistry and Biochemistry, Academy of Sciences of the Czech Republic, Prague 6, Czech Republic*

§*Institute of Biotechnology, University of Helsinki*

‖*Department of Global Health, College of Public Health*

⊥*University of South Florida*

#*MPI*

@*BioTechMed-Graz, Graz 8010, Austria*

△*School of Chemistry, University of Southamptaon, Southampton SO17 1BJ, United Kingdom*

▽*Chemical Biological and Radiological Sciences, Defence Science and Technology Laboratory, Porton Down, Salisbury, Wiltshire SP4 0JQ, United Kingdom*

E-mail: matti.javanainen@helsinki.fi; samuli.ollila@helsinki.fi

Contents

S1 Simulation Details

The force field specific simulation parameters used for each force field are listed in Table S1. The parameter input files (`.mdp`) are provided in the Zenodo portal (links in the main text). For all simulations, we used an integration time step of 2 fs and the leap-frog integrator of GROMACS. The isothermal–isobaric (NPT) ensemble was used with a temperature of 298 K and a pressure of 1 bar. All simulations were 1 µs long, and trajectories were written every 1 ns. The P-LINCS constraint algorithm[1,2] was used for the bonds noted in Table S1. NMRlipids databank[3] ID numbers of simulations are given in table S2.

Table S1: Simulation parameters used for different force fields.

Parameter	**CHARMM36**	**Slipids**	**Lipid17**	**MacRog**
Neighbour list type	Verlet[4]	Verlet[4]	Verlet[4]	Verlet[4]
Long-range electrostatics	PME	PME	PME	PME
LJ cut-off	1.2 nm	1.4 nm	0.9 nm	1.0 nm
LJ modifier	Force switch 1.0–1.2 nm	–	–	–
Dispersion correction	–	Energy & pressure[5]	Energy & pressure[5]	Energy & pressure[5]
Thermostat	Nosé–Hoover[6,7]	Stochastic rescaling[8]	Nosé–Hoover[6,7]	Stochastic rescaling[8]
Time constant (T)	1 ps	0.5 ps	1 ps	0.1 ps
Coupling groups	Lipids & water	Lipids & water	Lipids & water	Lipids & water
Barostat	Parrinello–Rahman[9]	Berendsen[10]	Parrinello–Rahman[9]	Parrinello–Rahman[9]
Coupling type (P)	semi-isotropic	semi-isotropic	semi-isotropic	semi-isotropic
Time constant (P)	5 ps	10 ps	5 ps	4 ps
Compressibility	$4.5{\cdot}10^{-5}$ 1/bar	$4.5{\cdot}10^{-5}$ 1/bar	$4.5{\cdot}10^{-5}$ 1/bar	$4.5{\cdot}10^{-5}$ 1/bar
Constraints	Bonds with H	All bonds	Bonds with H	All bonds
Water model	TIPS3P[11]	TIP3P[12]	TIP3P[12]	TIP3P[12]
FF Source	CHARMM-GUI	CHARMM-GUI	CHARMM-GUI	Refs. 13 & 14
Parameter source	CHARMM-GUI	Slipids website	CHARMM-GUI	Refs. 13 & 14

Table S2: NMRlipids databank IDs of performed simulations.

CHARMM36

System	ID
1024POPC_128CHOL_57600SOL_298K	426
64POPC_3200SOL_298K	546
1024POPC_896CHOL_96000SOL_298K	543
64POPC_40CHOL_5200SOL_298K	620
64POPC_56CHOL_6000SOL_298K	91
1024POPC_416CHOL_72000SOL_298K	412
1024POPC_256CHOL_64000SOL_298K	88
256POPC_64CHOL_16000SOL_298K	72
64POPC_8CHOL_3600SOL_298K	109
256POPC_104CHOL_18000SOL_298K	298
64POPC_16CHOL_4000SOL_298K	525
64POPC_26CHOL_4500SOL_298K	393
1024POPC_640CHOL_83200SOL_298K	550
256POPC_160CHOL_20800SOL_298K	275
256POPC_224CHOL_24000SOL_298K	166
256POPC_32CHOL_14400SOL_298K	119

Slipids

System	ID
Slipids_POPC_CHOL20_L	691
Slipids_POPC_CHOL47_M	712
Slipids_POPC_CHOL29_S	693
Slipids_POPC_CHOL20_S	692
Slipids_POPC_CHOL20_M	687
Slipids_POPC_CHOL11_S	672
Slipids_POPC_CHOL11_M	681
Slipids_POPC_L	696
Slipids_POPC_CHOL38_S	661
Slipids_POPC_M	708
Slipids_POPC_CHOL38_L	670
Slipids_POPC_S	664
Slipids_POPC_CHOL29_L	709
Slipids_POPC_CHOL29_M	659
Slipids_POPC_CHOL11_L	697
Slipids_POPC_CHOL38_M	668
Slipids_POPC_CHOL47_S	703
Slipids_POPC_CHOL47_L	682

Lipid17

System	ID
Lipid17_POPC_CHOL29_M	700
Lipid17_POPC_CHOL47_L	717
Lipid17_POPC_CHOL11_L	663
Lipid17_POPC_CHOL29_L	683
Lipid17_POPC_CHOL20_S	662
Lipid17_POPC_CHOL47_M	714
Lipid17_POPC_CHOL38_S	688
Lipid17_POPC_L	684
Lipid17_POPC_S	715
Lipid17_POPC_CHOL20_M	666
Lipid17_POPC_M	657
Lipid17_POPC_CHOL29_S	686
Lipid17_POPC_CHOL38_L	673
Lipid17_POPC_CHOL47_S	707
Lipid17_POPC_CHOL11_S	680
Lipid17_POPC_CHOL20_L	667
Lipid17_POPC_CHOL38_M	694
Lipid17_POPC_CHOL11_M	689

MacRog

System	ID
MacRog_POPC_CHOL38_S	716
MacRog_POPC_CHOL29_L	705
MacRog_POPC_CHOL47_M	699
MacRog_POPC_CHOL47_L	671
MacRog_POPC_CHOL20_L	677
MacRog_POPC_S	674
MacRog_POPC_CHOL20_M	706
MacRog_POPC_CHOL38_L	698
MacRog_POPC_CHOL38_M	679
MacRog_POPC_M	675
MacRog_POPC_L	658
MacRog_POPC_CHOL29_M	655
MacRog_POPC_CHOL11_L	660
MacRog_POPC_CHOL11_S	665
MacRog_POPC_CHOL29_S	690
MacRog_POPC_CHOL11_M	695
MacRog_POPC_CHOL47_S	704
MacRog_POPC_CHOL20_S	702

S2 Additional Results

S2.1 Scattering Intensities

S2.2 Form Factors & Electron Density Profiles

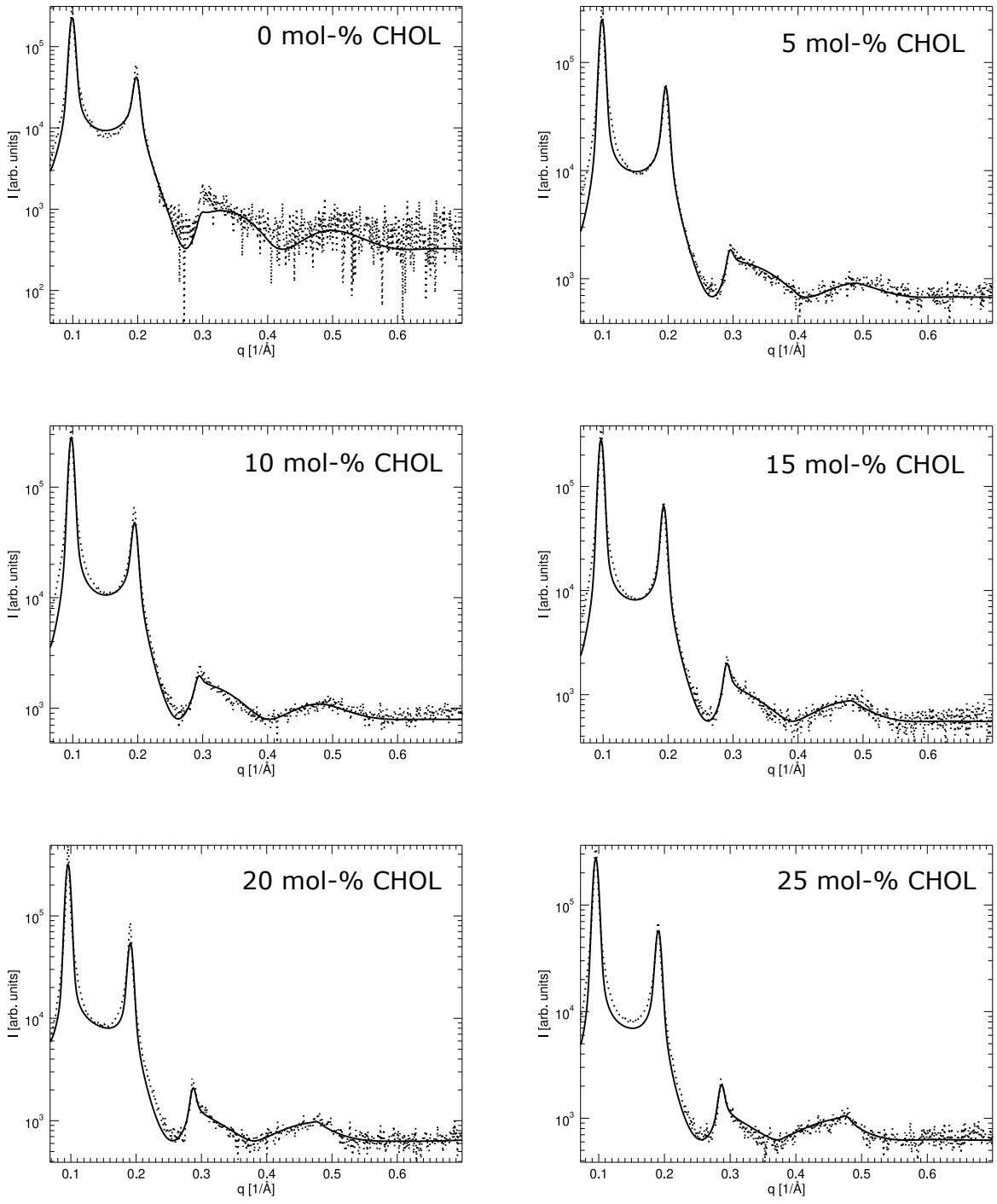

Figure S1: Scattering intensities from X-ray scattering experiments with various concentrations of cholesterol. More data are shown in the next figure.

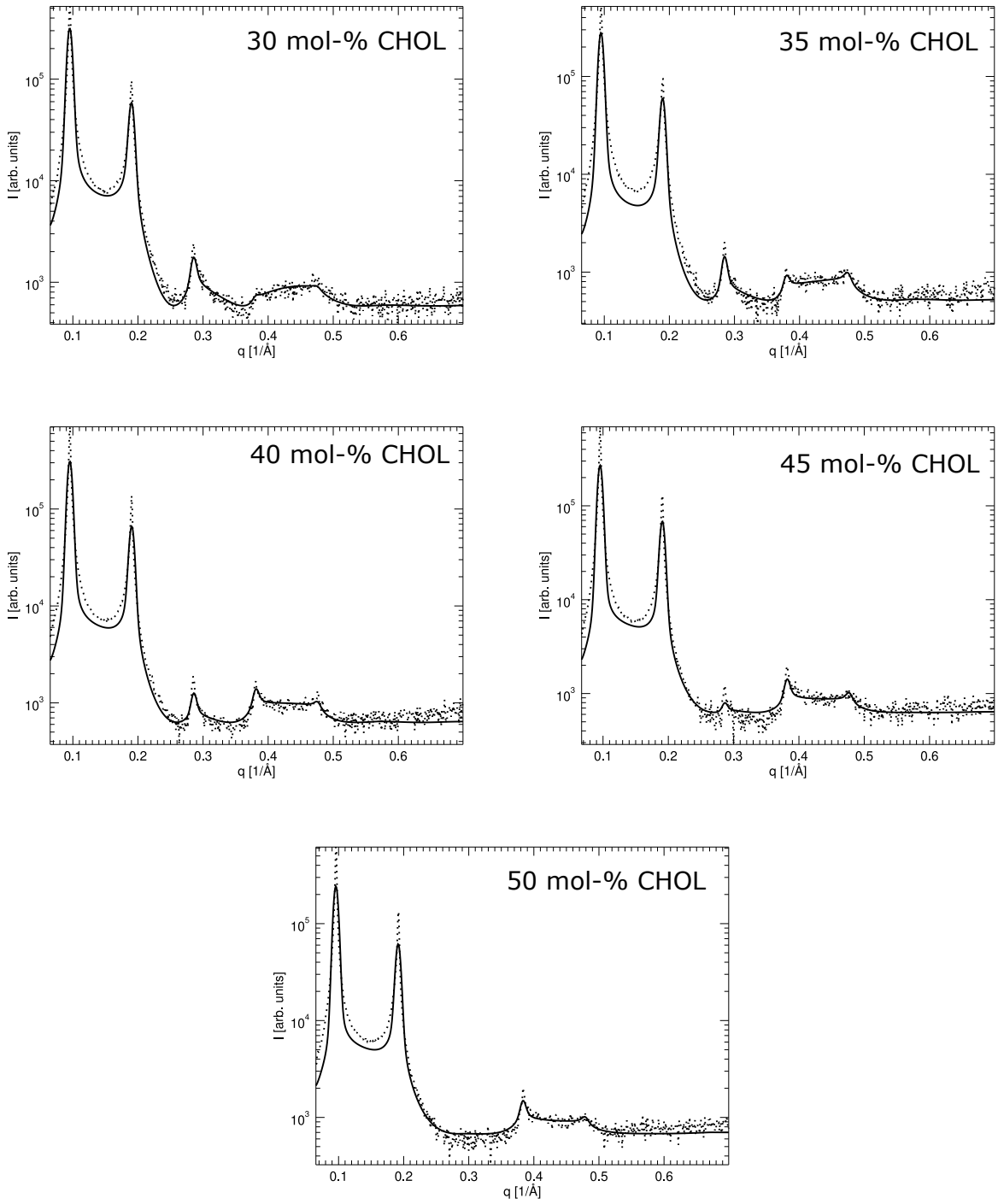

Figure S2: Scattering intensities from X-ray scattering experiments with various concentrations of cholesterol. More data are shown in the previous figure.

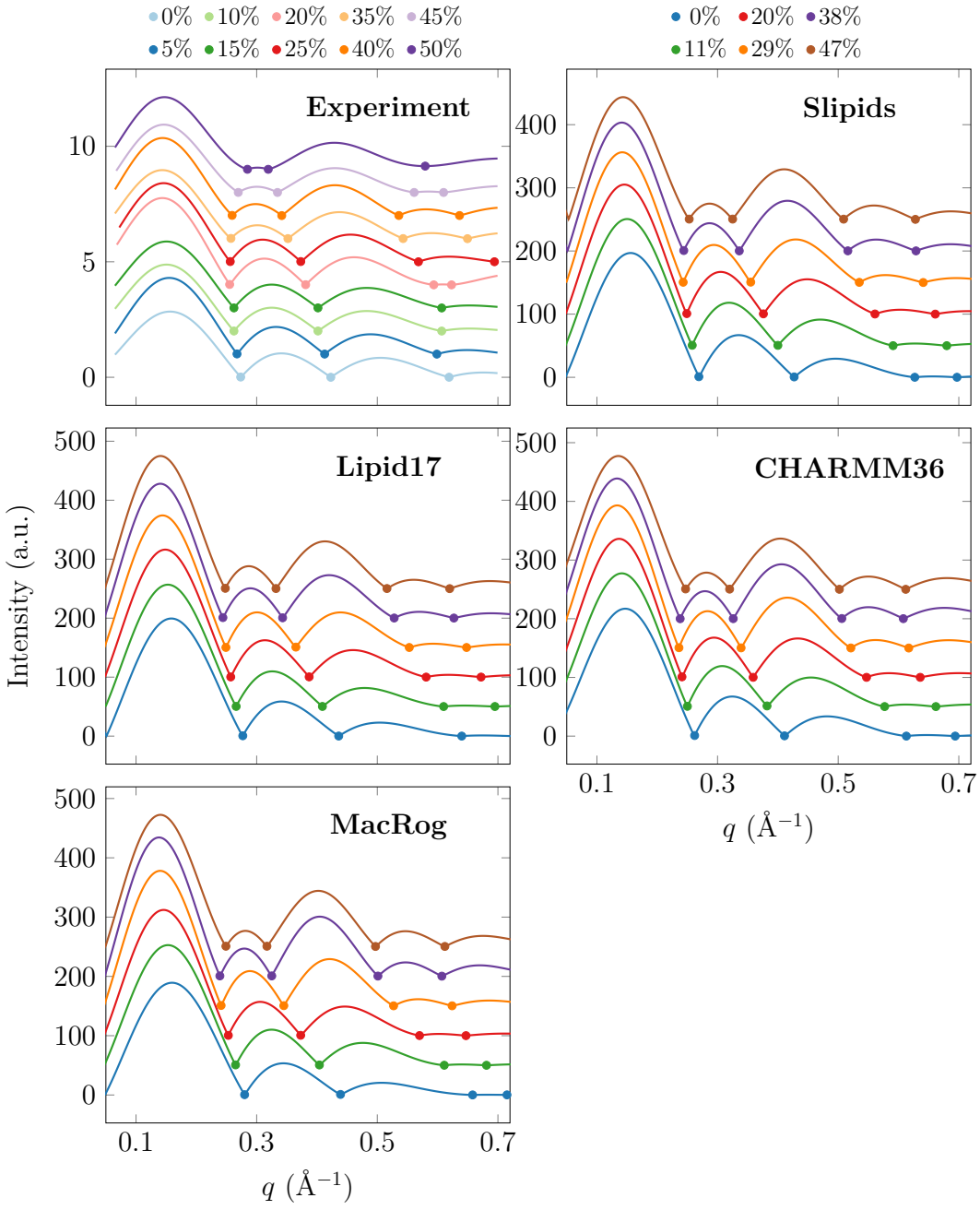

Figure S3: **Scattering intensities as a function of scattering vector from experiments and simulations.** Each of the profiles is shifted vertically with respect to the previous one, by 1 for the experimental profiles and by 50 for the computational ones. The minima are marked by filled circles to guide the eye.

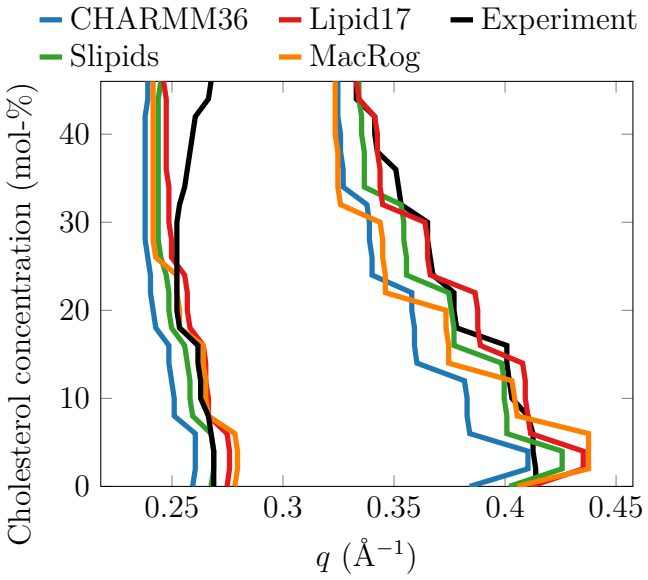

Figure S4: **Effecf of CHOL on the location of the first two minima in the form factor.** The minima are extracted from the form factors interpolated to all CHOL concentrations (Fig. S3) from experiment and simulation with the `findpeaks` function in Matlab.

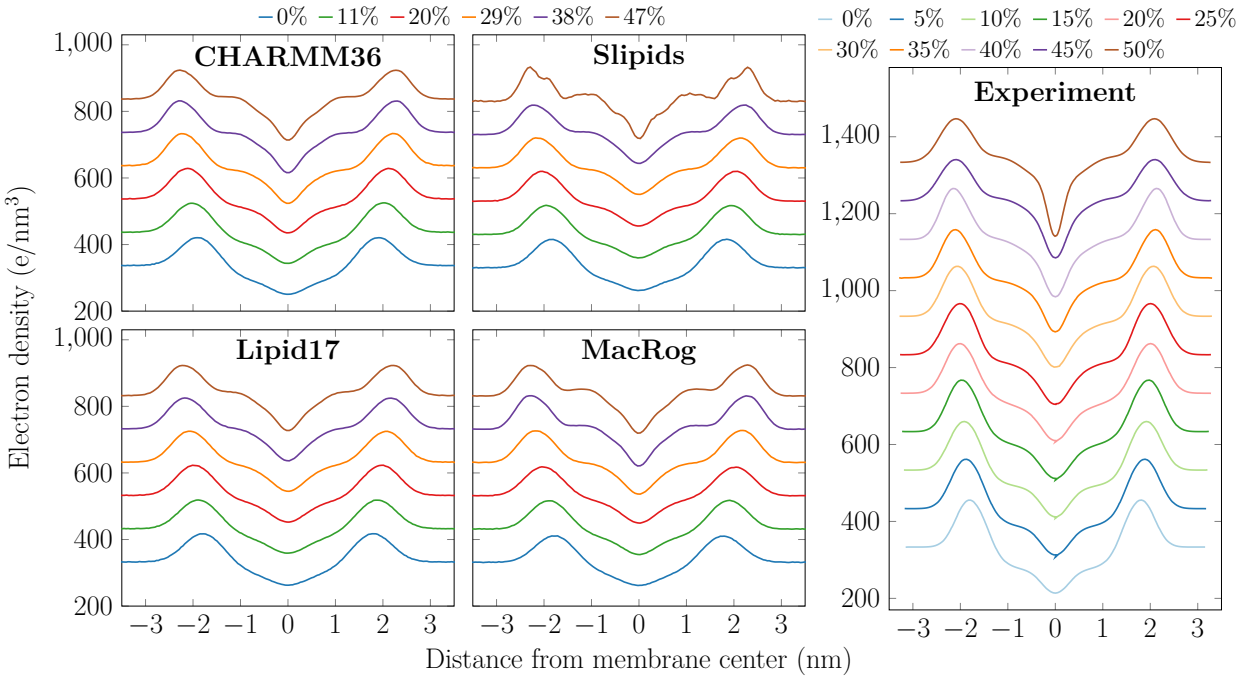

Figure S5: **Electron density profiles.** Each of the profiles is shifted vertically with respect to the previous one by 100 units.

S2.3 Order Parameters

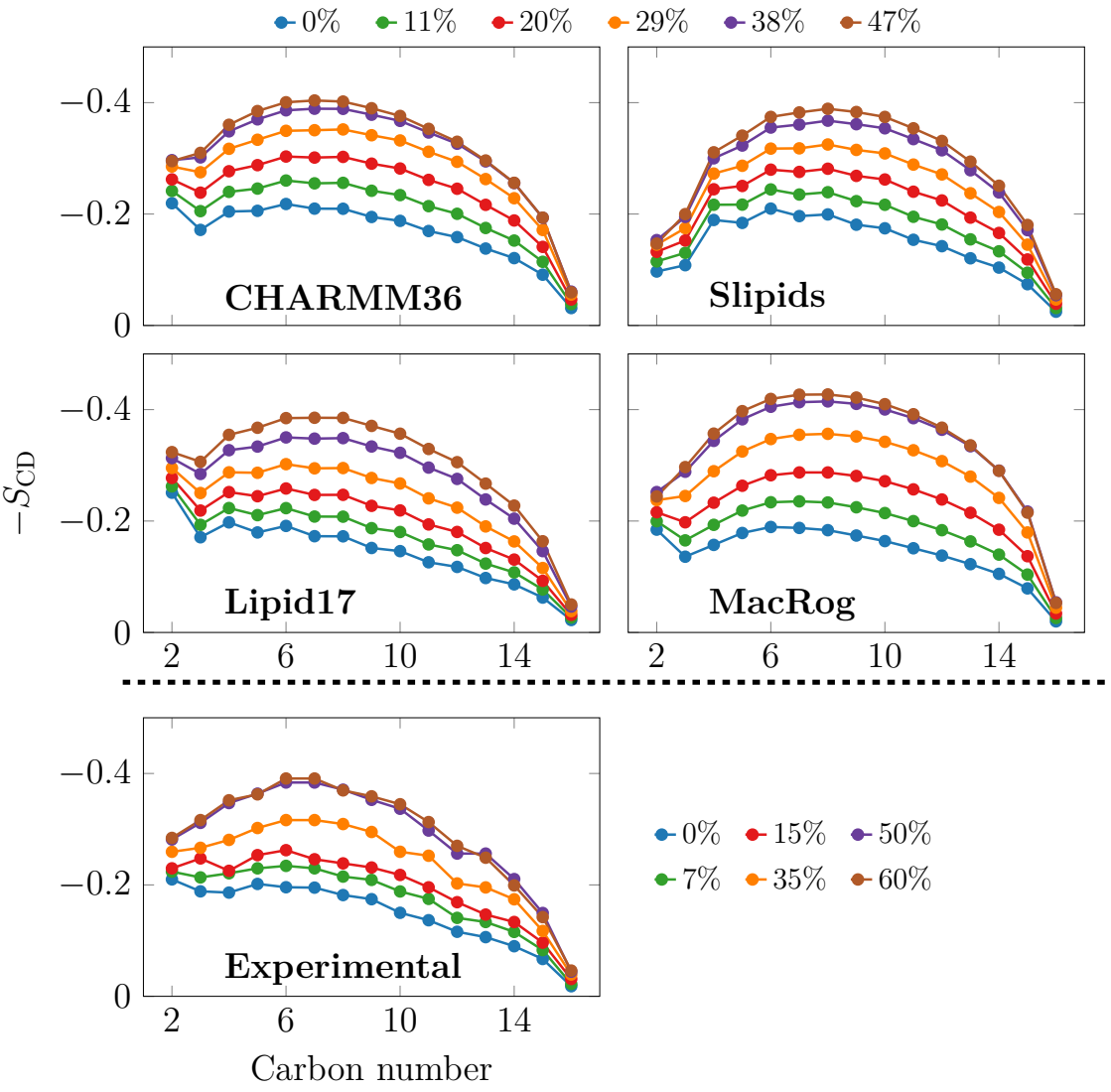

Figure S6: **Effect of cholesterol on the acyl chain order parameters of the POPC *sn*-1 (palmitate) chain.** The legend at the top corresponds to all simulations, and the one at the bottom to the experiments.

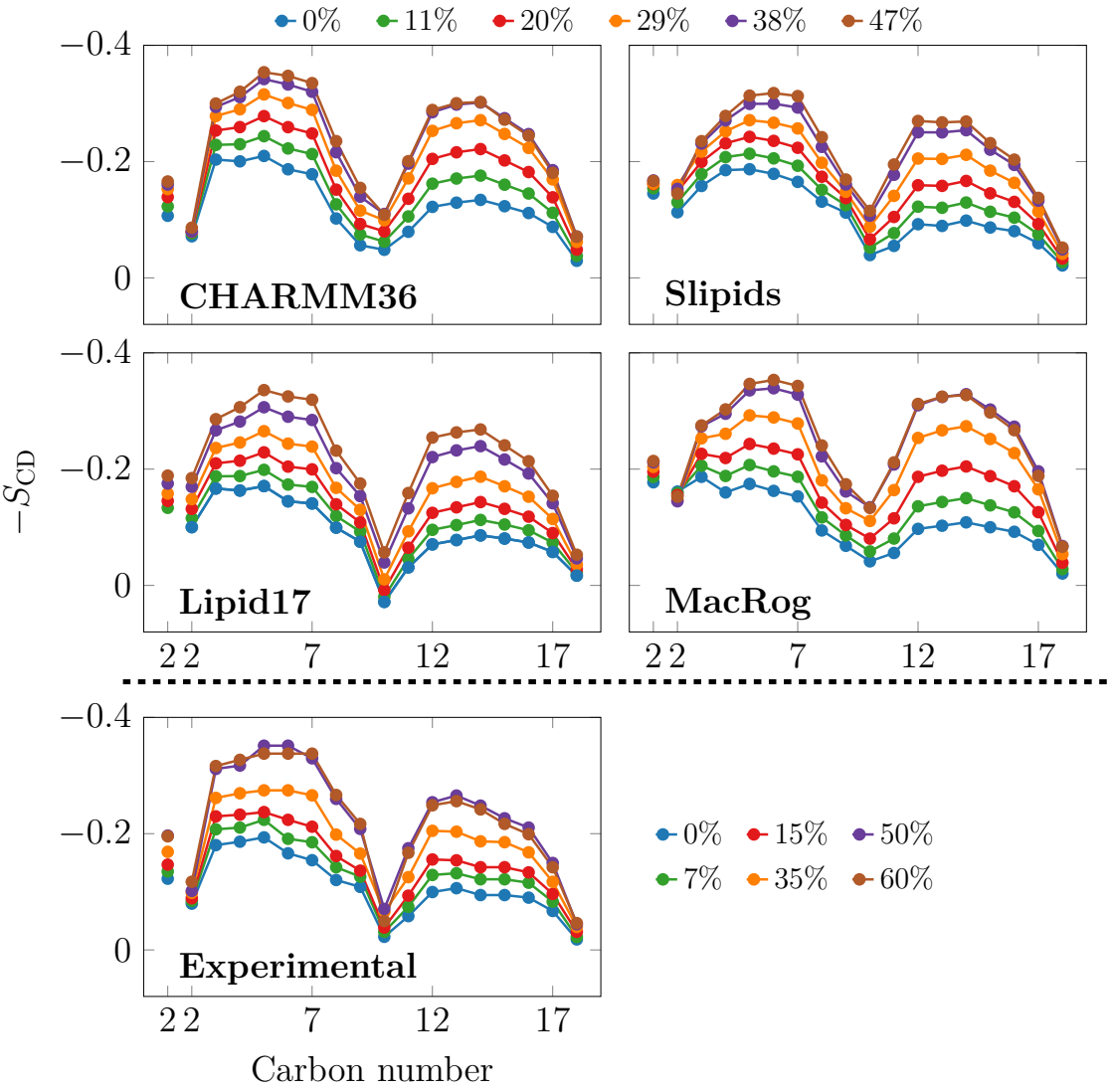

Figure S7: **Effect of cholesterol on the acyl chain order parameters of the POPC *sn*-2 (oleate) chain.** The legend at the top corresponds to all simulations, and the one at the bottom to the experiments. Since the order parameters measured for the two hydrogens bound to the C2 carbon differ, they are both shown in the plots.

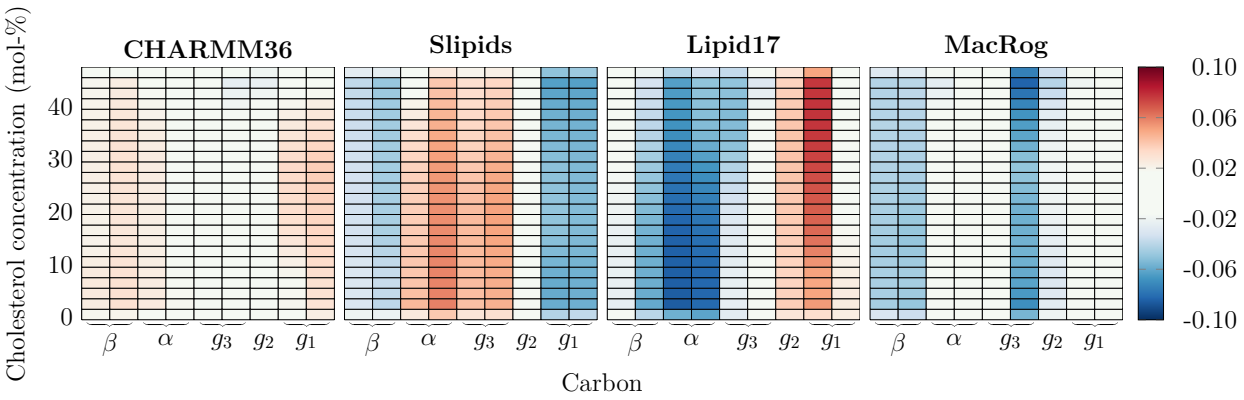

Figure S8: **The deviation of POPC head group parameters from experimental values as a function of CHOL concentration.**

S2.4 Dynamic Properties

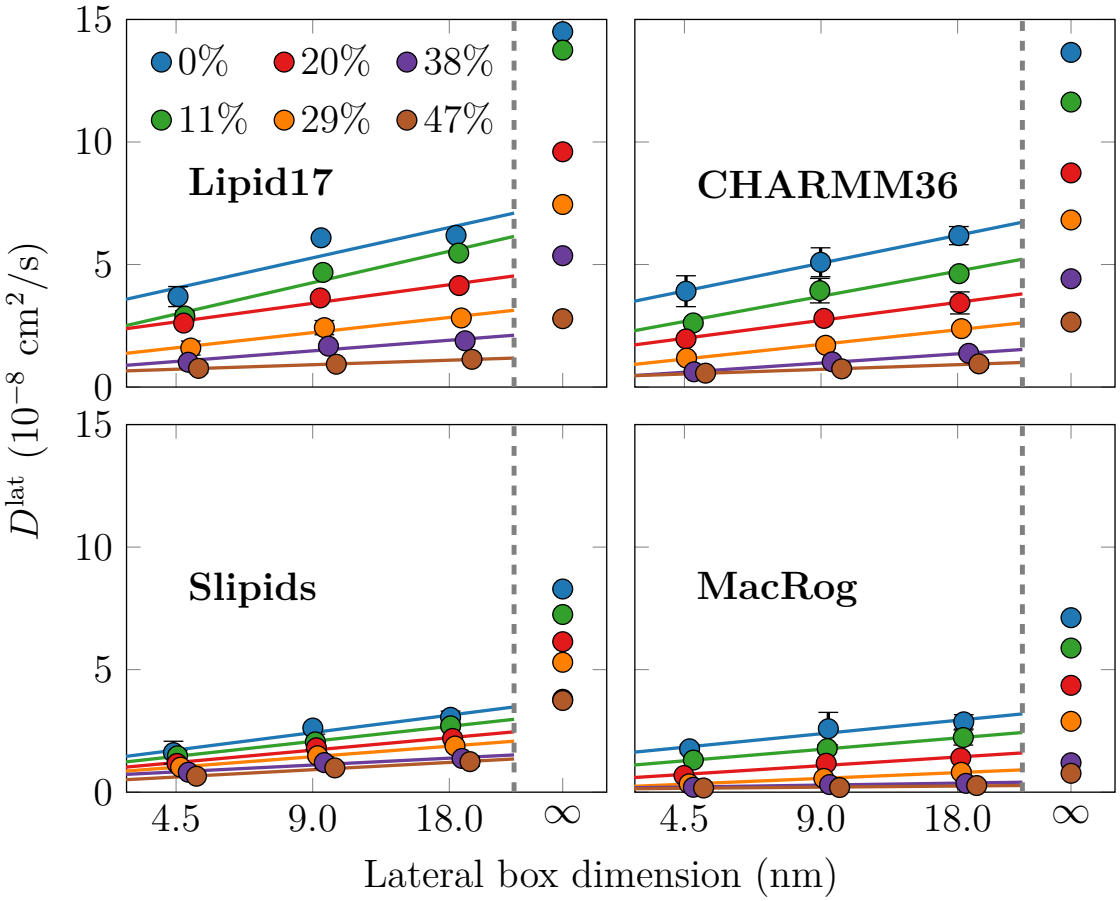

Figure S9: **Dependence of lateral diffusion coefficients on simulation box size.** The values calculated for the lipid centres of mass with `gmx msd` after eliminating leaflet drift. The values for the three system sizes are shown as markers together with fits of Eq. (**??**). The values extrapolated to infinite system sizes are also shown in the separate column.

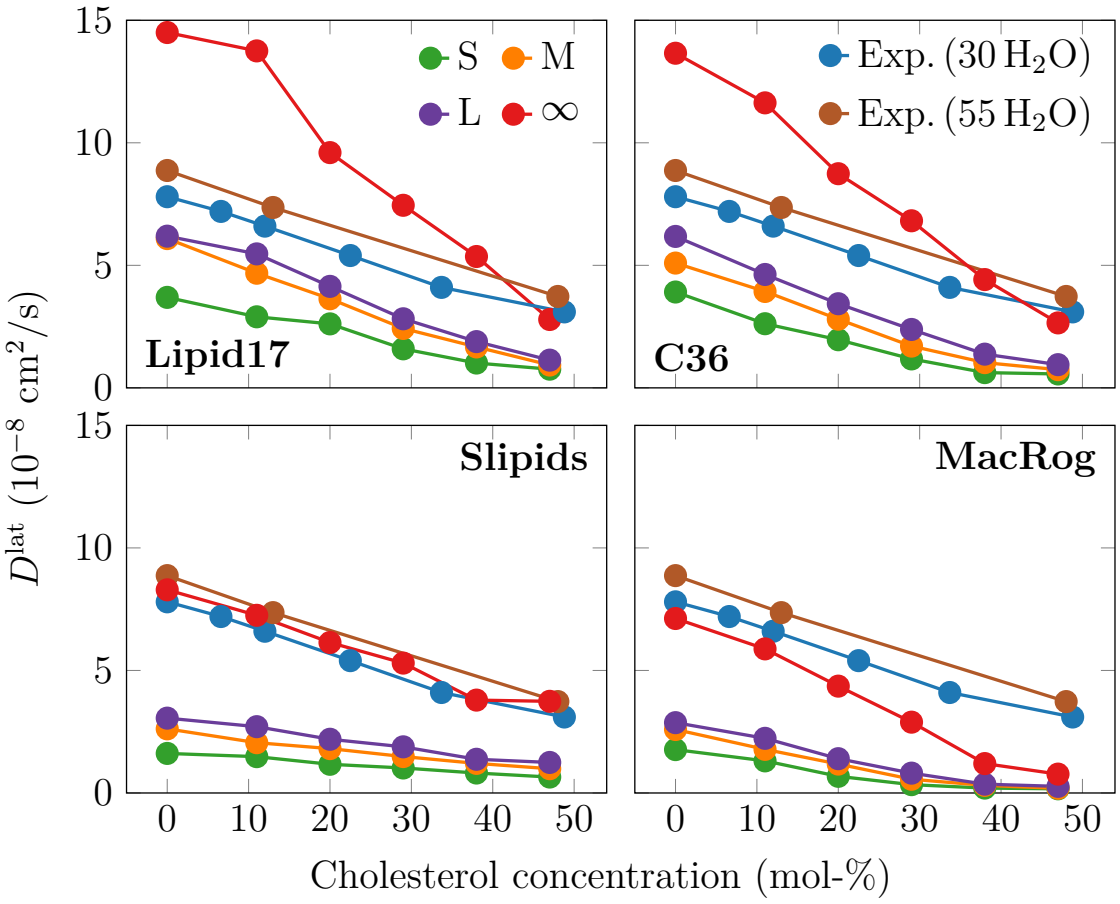

Figure S10: **Dependence of lateral diffusion coefficients on cholesterol concentration.** Data are shown for all system sizes; small (S), medium (M), and large (L). The values extrapolated to infinity are shown as well (∞). Experimental measured at two hydration levels, 30 m-% and 55-% of water.[15,16]

S2.5 Finite-Size Effects

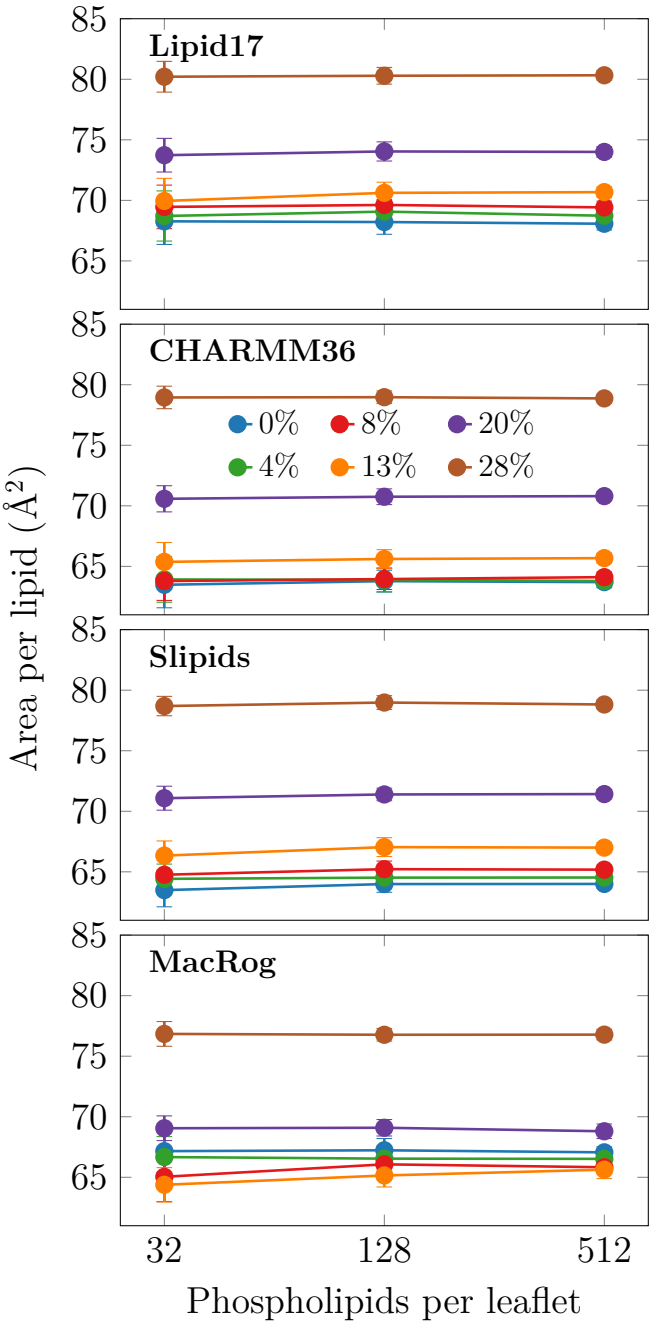

Figure S11: **Dependence of area per lipid on simulation box size.** Area per lipid is calculated by dividing the membrane area by the number of lipids in one leaflet. Error bars show standard error extracted using block averaging in `gmx analyze`.

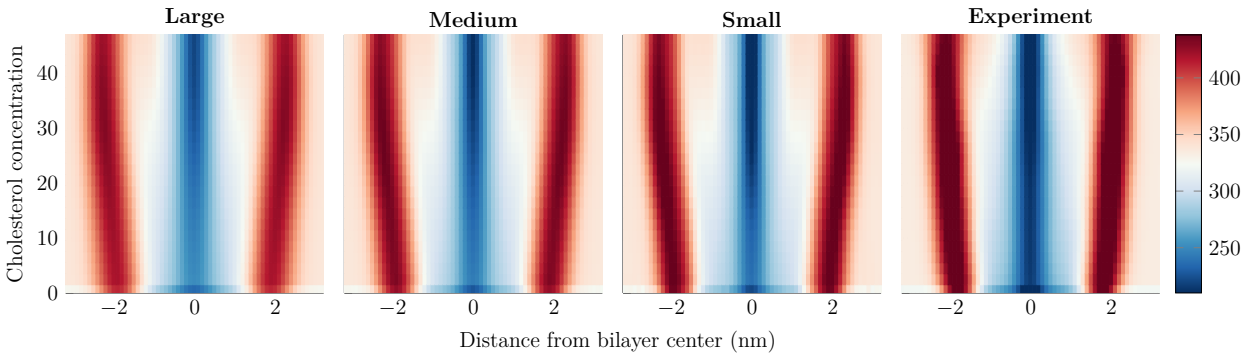

Figure S12: **Effect of system size on the density profiles.** Membrane undulations are larger in the larger systems, which leads to the smearing of the electron density profiles. Here, data are shown for CHARMM36 in the large (1024 POPC in total), medium (256 POPC in total), or small (64 POPC in total) systems. The experimental electron density profile is shown for comparison.

S2.6 Cholesterol Tilt

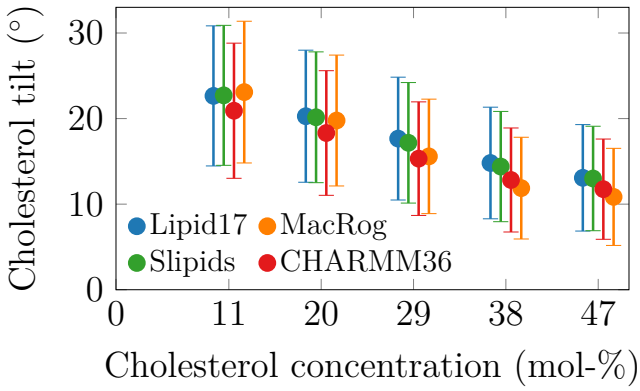

Figure S13: **Effect of cholesterol concentration on the tilt of the cholesterol molecules.** The tilt is defined as the angle between the vector connecting the C3 and C17 carbons at the two ends of the rigid ring structure of cholesterol. The hydroxyl group is bound to C3 and the hydrocarbon chain to C17. The tilt distributions were gathered from the two leaflets, fitted with a Gamma distribution, and the mean values and standard deviations were extracted and shown here as the value and error estimate, respectively. The cholesterol concentration was identical between the simulations, but the points are horizontally slightly shifted for clarity.

References

(1) Hess, B.; Bekker, H.; Berendsen, H. J. C.; Fraaije, J. G. E. M. LINCS: a linear constraint solver for molecular dynamics simulations. *J. Comput. Chem.* **1997**, *18*, 1463–1472.

(2) Hess, B. P-LINCS: A Parallel Linear Constraint Solver for Molecular Simulation. *J. Chem. Theory Comput.* **2008**, *4*, 116–122.

(3) Kiirikki, A. M.; Antila, H. S.; Bort, L.; Buslaev, P.; Favela, F.; Ferreira, T. M.; Fuchs, P. F.; Garcia-Fandino, R.; Gushchin, I.; Kav, B. et al. NMRlipids Databank: Making data-driven analyses of membrane properties accessible for all. 2023; `https://doi.org/10.26434/chemrxiv-2023-jrpwm`.

(4) Páll, S.; Hess, B. A flexible algorithm for calculating pair interactions on SIMD architectures. *Computer Physics Communications* **2013**, *184*, 2641–2650.

(5) Shirts, M. R.; Mobley, D. L.; Chodera, J. D.; Pande, V. S. Accurate and efficient corrections for missing dispersion interactions in molecular simulations. *The journal of physical chemistry B* **2007**, *111*, 13052–13063.

(6) Hoover, W. G. Canonical dynamics: Equilibrium phase-space distributions. *Phys. Rev. A* **1985**, *31*, 1695–1697.

(7) Nose, S. A molecular dynamics method for simulations in the canonical ensemble. *Mol. Phys.* **1984**, *52*, 255–268.

(8) Bussi, G.; Donadio, D.; Parrinello, M. Canonical sampling through velocity rescaling. *J. Chem. Phys.* **2007**, *126*.

(9) Parrinello, M.; Rahman, A. Polymorphic transitions in single crystals: A new molecular dynamics method. *Journal of Applied physics* **1981**, *52*, 7182–7190.

(10) Berendsen, H. J.; Postma, J. v.; Van Gunsteren, W. F.; DiNola, A.; Haak, J. R. Molecular dynamics with coupling to an external bath. *The Journal of chemical physics* **1984**, *81*, 3684–3690.

(11) Durell, S. R.; Brooks, B. R.; Ben-Naim, A. Solvent-induced forces between two hydrophilic groups. *The Journal of Physical Chemistry* **1994**, *98*, 2198–2202.

(12) Jorgensen, W. L.; Chandrasekhar, J.; Madura, J. D.; Impey, R. W.; Klein, M. L. Comparison of simple potential functions for simulating liquid water. *J. Chem. Phys.* **1983**, *79*, 926–935.

(13) Kulig, W.; Pasenkiewicz-Gierula, M.; Róg, T. Cis and trans unsaturated phosphatidylcholine bilayers: a molecular dynamics simulation study. *Chemistry and physics of lipids* **2016**, *195*, 12–20.

(14) Milan Rodriguez, P.; Fuchs, P. F. MacRog pure POPC MD simulation (300 K - 500ns - 1 bar). 2020; `https://doi.org/10.5281/zenodo.3741793`.

(15) Filippov, A.; Orädd, G.; Lindblom, G. The effect of cholesterol on the lateral diffusion of phospholipids in oriented bilayers. *Biophysical journal* **2003**, *84*, 3079–3086.

(16) Filippov, A.; Orädd, G.; Lindblom, G. Influence of cholesterol and water content on phospholipid lateral diffusion in bilayers. *Langmuir* **2003**, *19*, 6397–6400.